https://doi.org/10.5194/se-2019-119
Preprint. Discussion started: 10 July 2019

The formation of North-South Seismic Zone and Emeishan large igneous province in Western China: Insight from teleseismic tomography

Chuansong He[1, 2]

[1]*Institute of Geophysics, CEA, Beijing 100081, China*

[2]*Key Laboratory of Continental Collision and Plateau Uplift, Institute of Tibetan Plateau Research, Chinese Academy of Sciences, Beijing 100101, China*

Correspondence to: Chuansong He (hechuansong@aliyun.com)

https://doi.org/10.5194/se-2019-119
Preprint. Discussion started: 10 July 2019

Solid Earth Discussions

Abstract. Several models have been suggested to explain the earthquake mechanism of the North-South Seismic Zone (NSSZ) and the formation of the Emeishan Large Igneous Province (ELIP). In this study, I extended the study region and carried out detailed teleseismic tomography in the NSSZ and near-by regions. Results identified by this study reveal large plate-like high-velocity anomalies beneath the Songpan-Ganzi Block and the South China Block, which may be associated with large-scale lithospheric delamination, and low-velocity structures at 50-200 km depths in the western and southern parts of this study region, which imply upwelling asthenosphere induced by delamination and the absence of the rigid lithosphere there. Two high-velocity structures beneath the Sichuan Basin and the Alashan Block are revealed, which might be the lithospheric roots of these structures. These rigid lithospheric roots obstructed the eastward extrusion of the Tibetan Plateau and led to stress accumulations and releases (earthquakes) in the Longmenshan Orogenic Belt and the northern part of the NSSZ. Due to obstruction by the Sichuan Basin's lithosphere, eastward extrusion was redirected southeastward to Yunnan in the southern part of the NSSZ, which led to stress accumulations and releases (earthquakes) along the Honghe and Xiaojiang Faults. This study provide velocity images reveal a slab-like high-velocity structure, which might be associated with the lithospheric vestige of the Paleo-Tethys Ocean that subducted beneath the ELIP, which resulted in large-scale return mantle flow or mantle upwelling and contribute to the LIP formation in early Mesozoic.

Keywords: North-South Seismic Zone, Emeishan large igneous province, delamination of the lower crust/lithosphere, upwelling asthenosphere, subducted slab, tomography.

https://doi.org/10.5194/se-2019-119
Preprint. Discussion started: 10 July 2019

Solid Earth
Discussions

1. Introduction

The North-South Seismic Zone (NSSZ) is a region of high seismic hazard in China due to devastating earthquakes (Zhang et al., 2003; Deng et al., 2003), which are located in regions where multiple blocks amalgamate (Zhang, 2013; Wang et al., 2011; He et al., 2014b) (Fig. 1). The NSSZ is also a boundary between the highland in the western part and lowland in the eastern part of China and a north-south-trending gravity anomaly zone (Zhang, 2013). Given the documented historical earthquakes, more than one-third of strong earthquakes (magnitude over 7) in China have occurred in the NSSZ (Zhang et al., 2003; Deng et al., 2003).

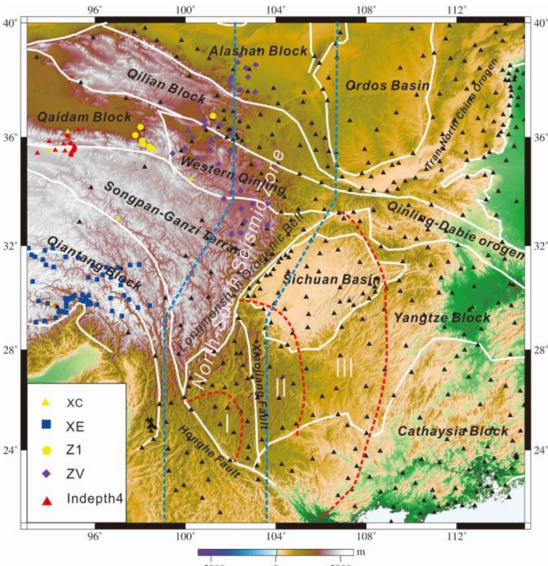

Figure 1. Geological units and tectonic framework. Circles, triangles, diamonds and rectangles: Seismic stations. I, II and III are the inner zone, intermediate zone and outer zone of the ELIP, respectively. Black dot lines indicate the North-South Seismic Zone (The figure was generated using the Generic Mapping Tool (http://gmt.soest.hawaii.edu/) provided by Chuansong He).

https://doi.org/10.5194/se-2019-119
Preprint. Discussion started: 10 July 2019

In China, the continental fragments or blocks collided and amalgamated during the Paleozoic to Mesozoic (Zhao X. et al., 2012; Lee and Lawver, 1995; Hodges, 2000; Rowley, 1998). During the Late Ordovician to Devonian, the Alashan Block and the North China Craton collided along the Qilian Orogenic Belt (Xu et al., 2006). During the Late Ordovician to Early Silurian, the Qilian and Qaidam Blocks amalgamated (Xu et al., 2006). In the Late Permian, the Songpan-Ganzi Block accreted to the Qaidam Block. During the Late Triassic to Early Jurassic, the Qiangtang Block amalgamated to the Songpan-Ganzi Block (Li et al., 2013; Zhang et al., 2004) along a Paleo-Tethyan suture. During the Late Jurassic, the Lhasa Block collided with the Qiangtang Block along the Neo-Tethyan suture (Li et al., 2013; Zhang et al., 2004) (Fig. 1). In the Mesozoic, North China Craton and South China Craton collision and assemble along the Sulu-Dabie-Qinling Orogen (Wu and Zheng, 2013; Yang et al., 2003; Dong et al., 2013). Finally, the major tectonic framework of China was formed, which includes the South China Craton (including the Yangtze Block and Cathaysia Block), North China Craton, Tarim Craton and the Tibetan Plateau.

The Tibetan Plateau includes the Songpan-Ganzi, Qiantang and Lhasa Blocks from north to south (Kapp et al., 2007; Zhu et al., 2011). The collision between the Indian and Eurasian Plates initiated from approximately 55 Ma (Chang et al., 1986; Zhang, 2001) and led to crustal shortening and thickening in the Alashan, Qilian, Qaidam, and Songpan-Ganzi Blocks and to east-west extrusion (Tapponnier et al., 2001).

The Permian-Triassic Emeishan large igneous province (ELIP) (Chung and Jahn, 1995) is located in the southern part of the NSSZ and is generally considered to have been generated by an upwelling mantle plume rooted in the core-mantle boundary (Ali et

https://doi.org/10.5194/se-2019-119
Preprint. Discussion started: 10 July 2019

al., 2010, Xiao et al., 2004). Based on the magma distribution, the ELIP is divided into 3 zones: inner zone, intermediate zone and outer zone (Ali et al., 2010; Xu et al., 2004) (Fig. 1).

To investigate the velocity structure of the crust/upper mantle and the earthquake mechanism of the NSSZ as well as the ELIP formation, a host of geophysical studies have been performed, such as deep seismic sounding (e.g., Li et al., 2002; Gao et al., 2006; Wang et al., 2014), shear-wave splitting (Wang et al., 2008), Pg and Sg tomography (Li et al., 2014), Pn tomography (Lei et al., 2014; Li Z.W. et al., 2012), noise tomography (Li et al., 2009, 2010; Bao et al., 2015), local tomography (Liu et al., 1989; Ding et al., 1999; Huang et al., 2009; Xu et al., 2012), P-wave tomography (Li et al., 2006; Yang et al., 2014; Bai et al., 2011; Huang et al., 2015; He et al., 2017; He and Santosh, 2017a, b), 2.5 dimensional tomography (Lü et al., 2014), and receiver functions (He et al., 2014a, b, c; Wu and Zhang, 2012; Hu et al., 2011, 2012).

Tomography has revealed prominent low-velocity layers in the middle crust under the eastern margin of the Tibetan Plateau (Li et al., 2009; Li et al., 2014); the Longmenshan Orogenic Belt is a boundary between the low- and high-velocity structures (Yang et al., 2014; Huang et al., 2015; He et al., 2019), and a Mesozoic deep process of large-scale delamination occurred in the western part of the Longmenshan Orogenic Belt (Bai et al., 2011; He et al., 2019). Receiver functions and tomography in the northeastern part of the Tibetan Plateau reveal an eastward subducted slab (Yang et al., 2014; Huang et al., 2015; He 2011; He et al., 2017a, b). Teleseismic tomography in the Longmenshan area has defined a large-scale high-velocity anomaly of plate-like appearance beneath the

https://doi.org/10.5194/se-2019-119
Preprint. Discussion started: 10 July 2019

Songpan-Ganzi Block (He et al., 2019), which is considered the delaminated rigid lithosphere of the Songpan-Ganzi Block. Receiver function and tomographic studies in the ELIP area have suggested that the ELIP was generated by upwelling asthenosphere, not an upwelling mantle plume rooted in the core-mantle boundary (He et al., 2014b, He and Santosh, 2017a).

However, recent tomographic studies indicate that large-scale low- and high-velocity anomalies cannot be well defined by relatively small-region tomography, and some important and large velocity structures should be further checked by relatively large-region tomography (Bastow, 2012; Chen et al., 2017). The results determined by receiver functions (such as delamination and upwelling mantle) need to be supported by velocity images. Therefore, I collected abundant teleseismic data recorded by temporary and permanent seismic stations in the NSSZ and near-by region, and carried out detailed tomography. Results identified by this study not only demonstrates a large-scale high-velocity anomaly of plate-like appearance beneath the Songpan-Ganzi Block at 400-500 km depth but also finds another large-scale high-velocity anomaly under the Yangtze and Cathaysia Blocks at 300-400 km depth. Images identified by this tomography show two large low-velocity structures at 50-200 km depth in the western and southern parts of the study region, which imply large-scale upwelling asthenosphere and the absence of the rigid lithosphere in these areas, which might be associated with the large-scale delamination.

2. Data and method

In this study, 585 teleseismic events collected from 513 permanent seismic stations

(China earthquake networks) and from Namche Barwa (XE, 60 temporary stations, Sol et al., 2007), the Tibetan Plateau Broadband Experiment (XC, 3 stations, 1991-1992), and the Northeast Tibet Seismic experiment (ZV, 36 stations, 2008-2010; Z1, 7 stations, 2006-2007). Epicentral distances of each station-event pair ranges between 30° and 85° with magnitudes larger than 6.0 (Fig. S1). Raw waveform with bandpass filtering between 0.3 and 3 Hz was cut 15 s before and 50 s after the first P-wave arrival. The time cross-correlation technique is used to pick 14492 P-wave arrival (VanDecar and Crosson, 1990). -3 s to +3 s traveltime residuals was limited to invert 3-D velocity model (Fig. S2).

An efficient 3-D ray-tracing technique was employed to calculate theoretical traveltimes and the ray paths (Zhao et al., 1992, 1994; Zhao, 2004). The large and sparse system of linear equations was determined by a conjugate-gradient algorithm (Paige and Saunders, 1982). I adopted 1° transverse grid, and 60, 100, 200, 300, 400, 500, 600, 700 and 800 km vertical grid and carried out crustal correction (designed 60 km crustal thickness) (Jiang et al., 2009, 2015) with the CRUST1.0 model (Laske et al., 2012). Following the L-shaped curve norm (Hansen, 1992; Lei and Zhao, 2007; Lei et al., 2009), 12.0 damping value was selected to invert 3-D velocity model (Fig. S3). I assigned ±2.5% velocity perturbations at all grid points and inverted the synthetic data. The checkerboard results show that the amplitude of the P-wave velocity perturbations are well recovered at almost all depth sections (Fig. S4).

3. Results

At 50, 100 and 200 km depths, the Hv1 and Hv2 high-velocity structures underlie the Ordos Basin and Sichuan Basin (Fig. 2), respectively. Li et al. (2006) and Bao et al.

https://doi.org/10.5194/se-2019-119
Preprint. Discussion started: 10 July 2019

(2015) also obtained similar results beneath the Ordos Basin and Sichuan Basin at 60-200 km depths and 95-155 km depths, respectively. The Lv1 low-velocity structure is located in the western part of the Longmenshan Orogenic Belt (Fig. 2), and the Lv2 low-velocity structure is located in the southern part of the Sichuan Basin (Fig. 2). Yang et al. (2014) and Huang et al. (2015) defined low-velocity structures at 70-300 km and 65-300 km depths in this area, respectively, which are similar to Lv1 and Lv2.

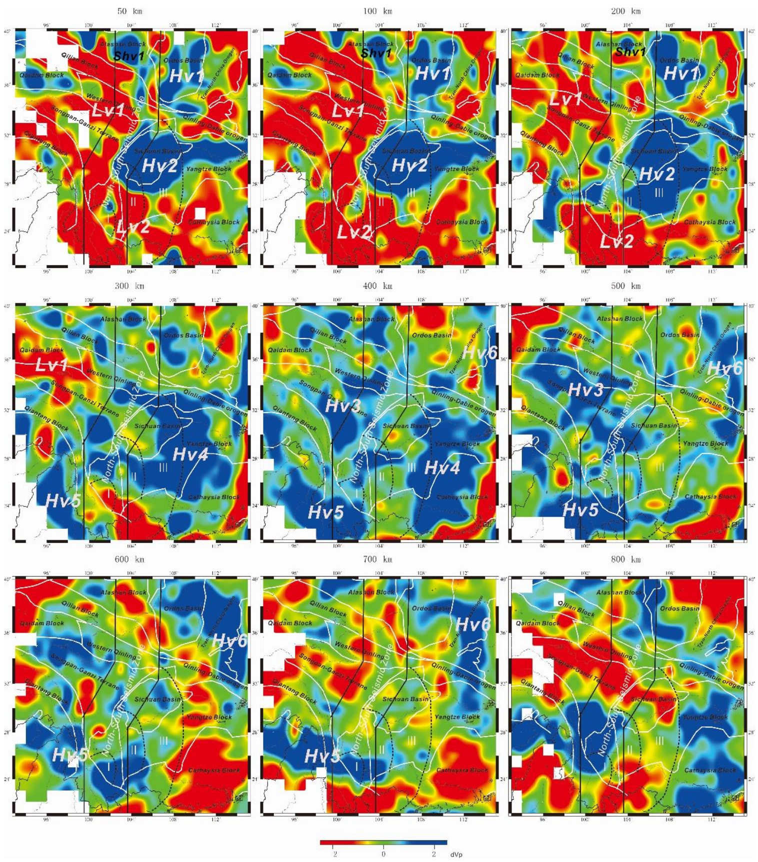

Figure 2. P-wave velocity perturbations at 50, 100, 200, 300, 400, 500, 600, 700 and 800 km depths. Portions of the model are not shown where the recovery from the input velocity model is below 20% (Fig. S4).

https://doi.org/10.5194/se-2019-119
Preprint. Discussion started: 10 July 2019

Solid Earth
Discussions
Open Access

At depths of 300 and 400 km, the Hv4 high-velocity anomaly underlies the Yangtze Block and Cathaysia Block (Fig. 2). Li et al. (2006) defined a similar high-velocity structure at a depth of 400 km. At depths of 400 and 500 km, the Hv3 high-velocity structure underlie the Songpan-Ganzi Block (Fig. 2). At depths of 400, 500, 600 and 700 km, the Hv5 and Hv6 high-velocity structure are located at the southeastern part and the eastern margin of the study region, respectively (Fig. 2). Huang et al. (2015) revealed a high-velocity anomaly at a depth of 300-700 km in the Chuandian area, and its location and scale are similar to Hv5.

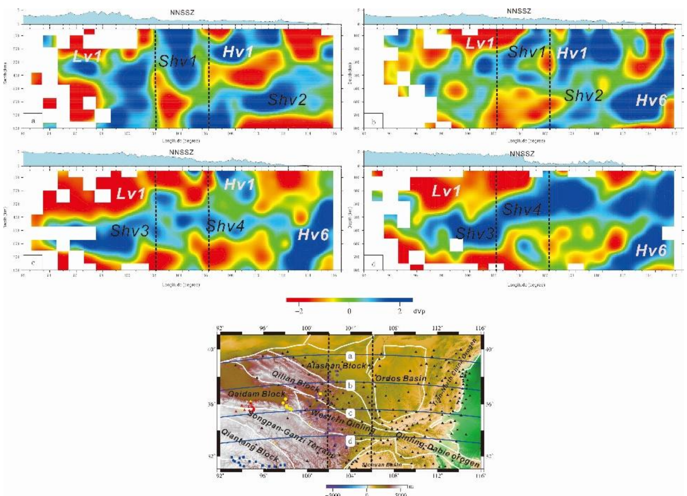

Figure 3. Profiles of P-wave velocity perturbations in the northern part of the NSSZ. Portions of the model are not shown where the recovery from the input velocity model is below 20% (Fig. S4) (The figure was generated using the Generic Mapping Tool (http://gmt.soest.hawaii.edu/) provided by Chuansong He).

In the northern part of the NSSZ, the western section has a low-velocity structure (Lv1), and the eastern part has a high-velocity structure (Shv1 or Hv1) (Fig. 3). Hv1 and SHv1 are under the Ordos Basin and Alashan Block, respectively, and might represent

https://doi.org/10.5194/se-2019-119
Preprint. Discussion started: 10 July 2019

the lithospheric roots of these structures. The Shv2, Shv3 and Shv4 high-velocity anomalies are located in the upper mantle transition zone at depths of 300-700 km. The Hv6 high-velocity structure is a subducted plate-like feature tilting from east to west. Based on its location and shape, I suggest that it is a Cenozoic subducted slab of the Pacific Plate (He and Zheng, 2018). Previous tomography indicated Hv1 and Lhv1 as well as high-velocity anomalies (Lhv2, Lhv3, Lhv4) in the upper mantle transition zone (Fig. S5) (He and Santosh, 2017b), which are consistent with this tomographic results (Fig. 3); however, a previous study did not reveal a clear lithospheric root for the Alashan Block, although the study also defined a high-velocity structure beneath the Alashan Block (Lhv1) (Fig. S5A) (He and Santosh, 2017b).

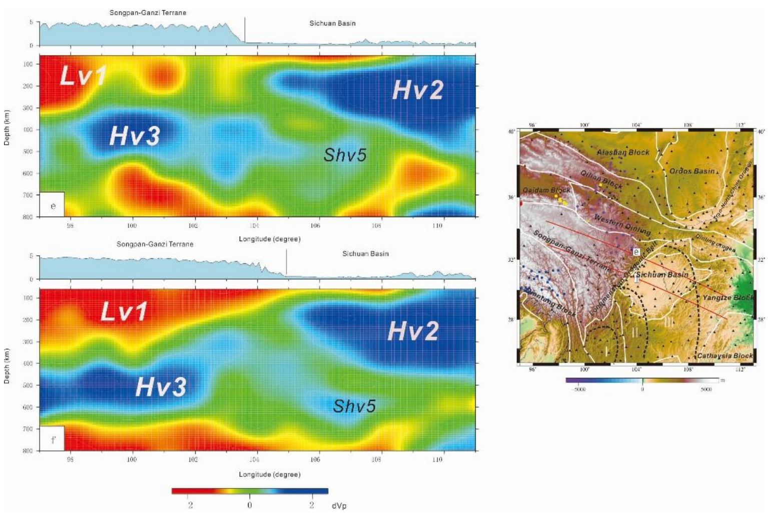

Figure 4. Profiles of P-wave velocity perturbations across the Longmenshan Orogenic Belt. Vertical lines: Longmenshan Orogenic Belt (The figure was generated using the Generic Mapping Tool (http://gmt.soest.hawaii.edu/) provided by Chuansong He).

In Fig. 4, the Longmenshan Orogenic Belt is a boundary between the low-velocity (Lv1) and high-velocity (Hv2) structures. Yang et al. (2014) and Huang et al. (2015) also

https://doi.org/10.5194/se-2019-119
Preprint. Discussion started: 10 July 2019

defined similar images. The plate-like high-velocity anomaly (Hv3) underlies the Songpan-Ganzi Block, and a small high-velocity anomaly (Shv5) underlies the Sichuan Basin (Fig. 4), which is consistent with the previous study (Fig. S6) (He et al., 2019).

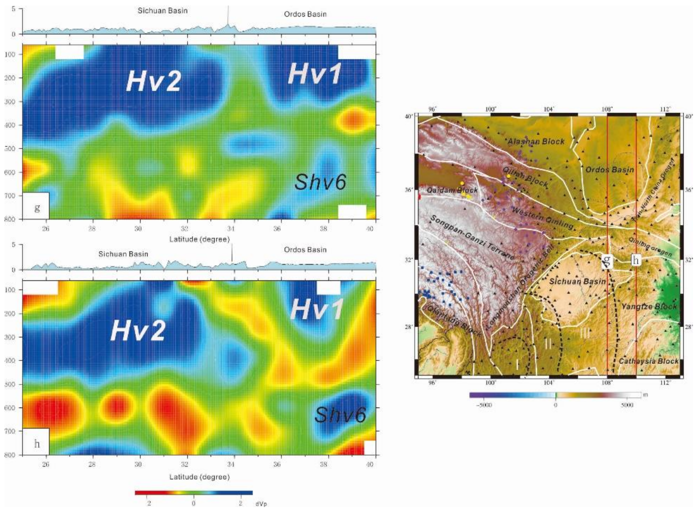

Figure 5. Profiles of P-wave velocity perturbations across the Ordos and Sichuan Basins. Portions of the model are not shown where the recovery from the input velocity model is below 20% (Fig. S4) (The figure was generated using the Generic Mapping Tool (http://gmt.soest.hawaii.edu/) provided by Chuansong He).

In Fig. 5, Hv1 and Hv2 underlie the Ordos Basin and Sichuan Basin, respectively. A small high-velocity anomaly (Shv6) is found under the Ordos Basin (Fig. 5); however, the scale of Shv6 is larger than that of Shv5 (Fig. 4, Fig. 5), and the thickness of Hv2 is greater than that of Hv1, which is also consistent with previous results (Fig. S7) (He et al., 2019).

https://doi.org/10.5194/se-2019-119
Preprint. Discussion started: 10 July 2019

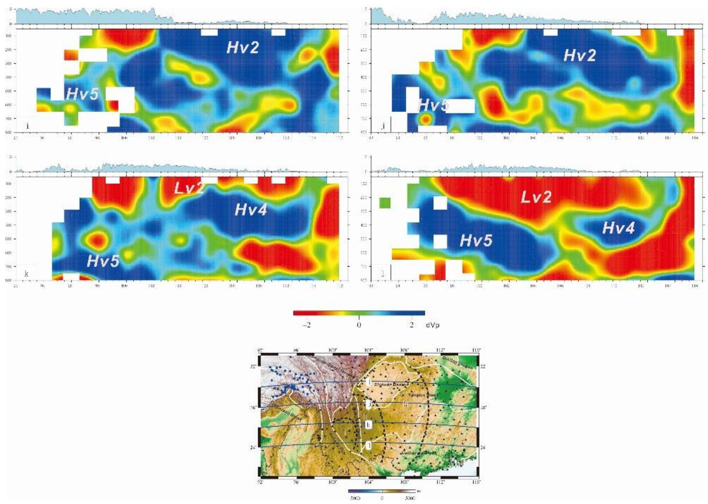

Figure 6. Profiles of P-wave velocity perturbations across the southern part of the NSSZ and ELIP. Portions of the model are not shown where the recovery from the input velocity model is below 20% (Fig. S4) (The figure was generated using the Generic Mapping Tool (http://gmt.soest.hawaii.edu/) provided by Chuansong He).

In Fig. 6, the Hv2 high-velocity structure underlies the Sichuan Basin (Fig. 6i, j), and a large low-velocity anomaly (Lv2) is found under the Yangtze and Cathaysia Blocks (Fig. 6k, l). Large plate-like high-velocity anomalies (Hv4) underlie the southern part of the study region (Fig. 6k, l). The Lv2 low-velocity anomaly identified by this study occurs in the upper mantle and is not rooted in the lower mantle. The Hv5 high-velocity structure resembles a subducted plate, and previous tomographic studies also revealed a similar velocity structure in this area (Huang et al., 2015; Yang et al., 2014; He et al., 2017a, b) (Fig. S8).

This tomography obtained new findings:

(1) I define a clear high-velocity structure of subducted plate-like appearance (Hv6) in the eastern margin of this study region.

https://doi.org/10.5194/se-2019-119
Preprint. Discussion started: 10 July 2019

(2) I reveal a lithospheric root for the Alashan Block.

(3) Two large low-velocity anomalies (Lv1 and Lv2) almost cover the eastern part and the southern part of the study region.

(4) A large low-velocity anomaly (Lv2) in the southern part of this study region occurs in the upper mantle and is not rooted in the lower mantle, which is different from previous tomographic images (He and Santosh, 2016; He and Santosh, 2017a).

(5) I not only define a large plate-like high-velocity anomaly (Hv3) beneath the Songpan-Ganzi Block but also find another large plate-like high-velocity anomaly (Hv4) under the Yangtze and Cathaysia Blocks.

4. Discussion

4.1. Delamination, upwelling asthenosphere and earthquakes

The NSSZ is located in a multiconvergent regime that underwent multistage collision and assembly from the Paleozoic to Mesozoic, involving the Caledonian Orogeny (Xu et al., 2006), Indosinian Orogeny and Himalayan Orogeny (Replumaz et al., 2010), accompanied by crustal compression and thickening (Tapponnier et al., 2001) due to collision and amalgamation of multiple blocks during the Paleozoic to Mesozoic.

Crustal thickening led to the transformation of granulite into eclogite (or to a density increase) in the lower crust, resulting in gravity instability and triggering delamination of the lower crust/lithosphere (Kay and Kay, 1993; Rudnick, 1995; Xu et al., 2013). Generally, delamination occurred simultaneously or after collision associated with an orogeny (Ueda et al., 2012). Delamination is also a major deep process for recycling lower crust/lithospheric mantle back into the Earth’s interior, which can lead to

https://doi.org/10.5194/se-2019-119
Preprint. Discussion started: 10 July 2019

heterogeneities in the mantle of velocity structure (Kay and Kay, 1993; Rudnick, 1995; Xu et al., 2013; He et al., 2019).

The low Vp/Vs ratio implies deep processes of lower crustal/lithospheric delamination in the northern part of the NSSZ and the ELIP (He et al., 2014a, b) (Figs. S9, S10). Previous receiver functions indicated that the lower crustal/lithospheric component delaminated into the upper mantle transition zone in the northern part of the NSSZ and the ELIP, which led to shallowing of both the 410 and 660 km discontinuities (Fig. S11, Fig. S12) (He et al., 2014a). A large high-velocity anomaly (Hv3) 200 km thick is found under the Songpan-Ganzi Block at 400-500 km depths, and another large-scale high-velocity anomaly (Hv4) 200 km thick lies beneath the Yangtze and Cathaysia Blocks at 300-400 km depths, which may be the lower crust/lithospheric mantle delaminated into the upper mantle or mantle transition zone. In the northern part of the NSSZ, Shv2, Shv3 and Shv4 are located in the mantle transition zone, and these high-velocity anomalies may be associated with delamination of the lower crust/lithospheric mantle. Delamination can result in upwelling asthenosphere that fills the void formed by delamination (Kay and Kay, 1993). Lv1 and Lv2 are above Hv3 and Hv4 (Fig. 2), respectively. Due to their well-defined correspondence, I consider the Lv1 and Lv2 to contribute upwelling asthenosphere that filled voids formed by delamination (Hv3 and Hv4).

The large-scale low-velocity structure at 50-200 km depths in the western part of the Longmenshan Orogenic Belt and Alashan Block as well as the southern part of the Sichuan Basin implies the absence of lithospheric mantle in these areas. The hot asthenosphere directly contacts and heats the lower crust (Anderson, 2007), which may

https://doi.org/10.5194/se-2019-119
Preprint. Discussion started: 10 July 2019

form a detachment surface between the lower crust and the top of the upper mantle, facilitating the easy eastward extrusion of the Tibetan Plateau. This process resulted in stress accumulations and releases (earthquakes) in the Longmenshan Orogenic Belt and the northern part of the NSSZ due to obstruction by the rigid lithosphere of the Sichuan Basin (He et al., 2019) and the Alashan Block.

In the southern part of the NSSZ, the seismicity shows that earthquakes are mainly controlled by the Honghe and Xiaojiang Faults (Xu et al., 2013). Geological studies have demonstrated that the eastward extrusion is redirected southeastward to Yunnan after obstruction by the rigid lithosphere of the Sichuan Basin (Clark and Royden, 2000; Royden et al., 2008), which may lead to stress accumulations and releases (earthquakes) in strike-slip faults such as the Honghe and Xiaojiang Faults that are not accommodated by east-west shortening along the margin of Tibet or western Sichuan and Yunnan (King, 1997). Accordingly, I consider the cause of the earthquakes in the southern part of the NSSZ to be different from those in other regions of the NSSZ.

Zhang (2003) also suggested interactions among the Chuandian, Songpan-Ganzi and South China Blocks, resulting in prominent tectonic deformation and earthquakes, such as the Wenchuan earthquake of 2008. The primary source of deformation comes from the eastward extrusion of the Tibetan Plateau blocked by the rigid lithosphere of the Sichuan Basin (e.g., Royden et al., 2008; Burchfiel et al., 2008).

4.2. ELIP formation

The cause of ELIP formation is not only important for understanding the dynamic trigger of other large igneous provinces in the world but also is relevant to the current debate surrounding the mantle plume theory (He et al., 2014b; Xu et al., 2007). Recently, the contribution and role of an upwelling mantle plume in the Emeishan flood basalts have been challenged (He et al., 2014b; He and Santosh, 2017a). The dynamic uplift in response to upwelling mantle plumes is very difficult to assess in many igneous provinces (Peate and Bryan, 2008). Silver (2006) proposed that such magmatic activity was induced by stress perturbations, not by upwelling mantle plumes rooted in the core-mantle boundary. Elkins-Tanton and Hager (2000) suggested that the preeruptive subsidence of the Siberian Traps flood basalts was associated with lower lithospheric delamination, which induced upwelling asthenosphere flowing into the voids formed by delamination.

Petrological and geological studies have suggested that voluminous continental flood basalts of the ELIP in SW China and northern Vietnam formed from the same upwelling mantle (Xu et al., 2004; Chung and Jahn, 1995). Northern Vietnam was located along the western part of the Honghe Fault in the Early Triassic; it was displaced several hundred kilometers to the southeast along the Ailao-Shan–Honghe Fault in the Oligo-Miocene (Ali et al., 2005). This situation implies that the ELIP was generated after the collision and amalgamation of the Indochina and South China Blocks in the Early Triassic along the Ailao-Shan-Honghe Fault-Song Ma suture.

Geological investigations and receiver function studies have suggested large-scale delamination of the crust/lithosphere following the convergence between the Yangtze and North China Cratons and the North Tibetan continental blocks in the Triassic (Zhang et al., 2008; He et al., 2014c). The large-scale delamination of the lower crust/lithospheric

https://doi.org/10.5194/se-2019-119
Preprint. Discussion started: 10 July 2019

mantle (Hv4) might induce large-scale upwelling asthenosphere (Lv2). At same time, the lower crust/lithospheric mantle (e.g., Hv4) delaminated into the upper mantle transition zone, dehydrated and formed plume-like mantle upwelling there (Lustrino, 2005; He et al., 2014b), which may also contribute to Lv2. Finally, the upwelling asthenosphere (Lv2) led to ELIP formation. New zircon U-Pb studies indicate that the Emeishan magmatism occurred between 257 and 260 Ma and was very short-lived (Shellnutt et al., 2012). An upwelling mantle plume is generally relatively long-lived (Pirajno, 2007). In contrast, delamination and the related upwelling of asthenosphere produce a relatively rapid event (Li S.Z. et al., 2012).

On the other hand, I define a slab-like high-velocity anomaly (Hv5) (Fig. 6), based on previous studies (Mo et al., 2001; Metcalfe, 2013), it might be a vestige of the subduction lithosphere of the Paleo-Tethys Ocean. The subducted slab can induce the return mantle flow and mantle upwelling in the mantle (Santosh et al., 2010; Zhao and Ohtani, 2009; Garfunkel, 1975), which possibly played an important role in the formation of the ELIP. The large-scale low-velocity (Lv2) anomaly identified by this study just is above Hv5. Therefore, I suggest there is a possibility that the Lv2 might be linked to the large-scale mantle return flow induced by the subducted slab of the Paleo-Tethys Ocean lithosphere.

5. Conclusions

It is suggested that large-scale delamination, generated by collision and amalgamation of multiple blocks during the Paleozoic to Mesozoic, may be a major deep process in the NSSZ. I consider that Hv3 and Hv4 should represent the delamination of the lower crust/lithosphere due to block collision and amalgamation. This process might contribute to the upwelling of the asthenosphere (Lv1 and Lv2) to fill voids formed by delamination, such as Hv3 and Hv4. The western and southern parts of the study region are covered by two large low-velocity structures (Lv1 and Lv2) at 50-200 km depths, which show the absence of the rigid lithosphere in these areas. Eastward extrusion is obstructed not only by the lithospheric root of the Sichuan and Ordos Basins but also by the lithospheric root of the Alashan Block, which leads to stress accumulations and releases (earthquakes) in the Longmenshan area and the northern part of the NSSZ. In the southern part of the NSSZ, the eastward extrusion is redirected southeastward along strike-slip faults such as the Honghe and Xiaojiang Faults, which results in stress accumulations and releases (earthquakes) on these faults. This study also indicates that the ELIP was generated by upwelling asthenosphere due to delamination induced by the collision and assemble between the terrane in early Mesozoic and the mantle return flow generated by the subducted slab of Paleo-Tethys Oceanic lithosphere, not by an upwelling mantle plume rooted in the core-mantle boundary.

Acknowledgments

Thanks to the Key Laboratory of Continental Collision and Plateau Uplift, Institute of Tibetan Plateau Research, Chinese Academy of Sciences (Grant No. LCPU201901). Waveform data for this study were provided by the Data Management Center of the China National Seismic Network at the Institute of Geophysics (SEISDMC, doi:10.11998/SeisDmc/SN) (http://www.seisdmc.ac.cn/), China Earthquake Networks Center.

References

Ali, J. R., Fitton, J. G., and Herzberg, C.: Emeishan large igneous province (SW China) and the mantle-plume up-doming hypothesis, J. Geol. Soc. Lond., 167, http://doi.org/10.1144/0016-76492009-129, 953-959, 2010.

Ali, J. R., Thompson, G. M., Zhou, M. F., and Song, X. Y.: Emeishan large igneous province, SW China, Lithos, 79, http://doi.org/10.1016/j.lithos.2004.09.013, 475-489, 2005.

Anderson, D. L.: Discussion of The Eclogite Engine: Chemical geodynamics as a Galileo thermometer, GSA Spec. Pap., 430, http://doi.org/10.1130/2007.2430(57), 47-64, 2007.

Bai, Z. M., Tian, X. B., and Tian, Y.: Upper mantle P-wave tomography across the Longmenshan fault belt from passive-source seismic observations along Aba-Longquanshan profile, J. Asian Earth Sci., 40, 873-882, http://doi.org/10.1016/j.jseaes.2010.04.036, 2011.

Bao, X. W., Song, X. D., and Li, J. T.: High-resolution lithospheric structure beneath Mainland China from ambient noise and earthquake surface-wave tomography, Earth Planet. Sc. Lett., 417, 132-141, http://doi.org/10.1016/j.epsl.2015.02.024, 2015.

Bastow, I. D.: Relative arrival-time upper-mantle tomography and the elusive background mean, Geophys. J. Int., 190, 1271-1278, http://doi.org/10.1111/j.1365-246x.2012.05559.x, 2012.

Burchfiel, B. C., Royden, L. H., van der Hilst, R. D., Hager, B. H., Chen, Z., King, R. W.,

https://doi.org/10.5194/se-2019-119
Preprint. Discussion started: 10 July 2019

Li, C., Lü, J., Yao, H., and Kirby, E.: A geological and geophysical context for the Wenchuan earthquake of 12 May 2008, Sichuan, People's Republic of China, GSA Today, 18, 4-11, http://doi.org/10.1130/GSATG18A.1, 2008.

Chang, C. F., Chen, N. S., Coward, M. P., Deng, W. M., Dewey, J. F., Gansser, A., Harris, N. B. W., Jin, C. W., Kidd, W. S. F., Leeder, M. R., Li, H. A., Lin, J. L., Liu, C. J., Mei, H. J., Molnar, P., Pan, Y., Pan, Y. S., Pearce, J. A., Shackleton R. M., Smith, A. B., Sun, Y. Y.， Ward, M., Watts, D. R., Xu, J. T., Xu, R. H., Yin, J. X., and Zhang, Y. Q.: Preliminary conclusions of the Royal Society and Academia Sinica 1985 geotraverse of Tibet, Nature, 323, 501-507, http://doi.org/10.1038/323501a0, 1986.

Chen, C., Zhao, D., Tian, Y., Wu, S. G., Hasegawa, A., Lei, J. S., Park, J. H., and Kang, I. B.: Mantle transition zone, stagnant slab and intraplate volcanism in Northeast Asia, Geophys. J. Int., 209, 68-85, http://doi.org/10.1093/gji/ggw491, 2017.

Chung, S. L., and Jahn, B. M.: Plume-lithosphere interaction in generation of the Emeishan flood basalts at the Permian-Triassic boundary, Geology, 23, 889-892, http://doi.org/10.1130/0091-7613(1995)023<0889:PLIIGO>2.3.CO;2, 1995.

Clark, M. K., and Royden, L. H.: Topographic ooze: building the eastern margin of Tibet by lower crustal flow, Geology, 28, 703-706, http://doi.org/10.1130/0091-7613(2000)28<703:TOBTEM>2.0.CO;2, 2000.

Data Management Centre of China National Seismic Network.: Waveform data of China National Seismic Network. Institute of Geophysics, China Earthquake Administration, http://www.seisdmc.ac.cn, doi:10.11998/SeisDmc/SN, 2007.

Deng, Q., Zhang, P., Ran, Y., Yang, X., Min, W., and Chu, Q.: Basic characteristics of

https://doi.org/10.5194/se-2019-119
Preprint. Discussion started: 10 July 2019

Solid Earth Discussions
Open Access
EGU

active tectonics of China, Sci. China Ser. D, 46, 356-372, http://doi.org/10.1360/03yd9032, 2003.

Ding, Z. F., He, Z. Q., Sun, W. G., and Sun, H. C.: 3-D crustal and upper mantle velocity structure in eastern Tibetan plateau and its surrounding area, Chinese J. Geophys., 42, 197-205, http://doi.org/10.1016/S0009-2541(98)00147-8, 1999.

Dong, S. W., Li, T. D., Lü, Q. T., Gao, R., Yang, J. S., Chen, X. H., Wei, W. B., and Zhou, Q.: SinoProbe team Progress in deep lithospheric exploration of the continental China: A review of the SinoProbe, Tectonophysics, 606, 1-13, http://doi.org/10.1016/j.tecto.2013.05.038, 2013.

Elkins-Tanton, L. T., and Hager, B. H.: Melt intrusion as a trigger for lithospheric foundering and the eruption of the Siberian flood basalts, Geophys. Res. Lett., 27, https://doi.org/3937-3940,10.1029/2000gl011751, 2000.

Garfunkel, Z.: Growth, Shrinking, and Long-Term Evolution of Plates and Their Implications for the Flow Pattern in the Mantle, J. Geophys. Res., 80, 4425-4432, https://doi.org/10.1029/JB080i032p04425, 1975.

Gao, R., Wang, H. Y., Ma, Y. S., Zhu, X., Li, Q. S., Li P. W., Kuang, Z. Y., and Lu, Z. W.: Tectonic Relationships between the Zoigê Basin of the Song-Pan Block and the West Qinling Orogen at Lithosphere Scale: Results of Deep Seismic Reflection Profiling, Act. Geosci. Sin., 27, 411-418, https://doi.org/10.3321/j.issn:1006-3021.2006.05.004, 2006.

Jiang, G. M., Zhang, G. B., Zhao, D., Lü, Q. T., Li, H. Y., and Li, X. F.: Mantle dynamics and Cretaceous magmatism in east-central China: Insight from teleseismic

https://doi.org/10.5194/se-2019-119
Preprint. Discussion started: 10 July 2019

tomograms, Tectonophysics, 664, 256-268, https://doi.org/10.1016/j.tecto.2015.09.019, 2015.

Jiang, G. M., Zhao, D. P., and Zhang, G. B.: Crustal correction in teleseismic tomography and its application, Chinese J. Geophys., Res. 52, 1508-1514, https://doi.org/10.3969/j.issn.0001-5733.2009.06.012, 2009.

Kapp, P., DeCelles, P. G., Gehrels, G. E., Heizler, M., and Ding, L.: Geological records of the Lhasa–Qiangtang and Indo–Asian collisions in the Nima area of central Tibet, Geol. Soc. Am. Bull., 119, 917-932, https://doi.org/10.1130/B26033, 2007.

Kay, R. W., and Kay, S. M.: Delamination and delamination magmatism, Tectonophysics, 219, 177-189, https://doi.org/10.1016/0040-1951(93)90295-U, 1993.

Kennett, B., and Engdahl, E.: Traveltimes for global earthquake location and phase identification, Geophys. J. Int., 105, 429-465, https://doi.org/10.1111/j.1365-246X.1991.tb06724.x, 1991.

King, R. W.: Geodetic measurement of crustal motion in southwest China, Geology, 25, 179-182, https://doi.org/10.1130/0091-7613(1997)025<0179:GMOCMI>2.3.CO;2, 1997.

Hansen, P.: Analysis of discrete ill-posed problems by means of the L-curve, SIAM Rev., 34, 561-580, https://doi.org/10.2307/2132628, 1992.

He, C. S.: Seismic evidence for plume and subducting slab in West Yunnan, Southwestern China, Act. Geol. Sin., 85, 629-636, https://doi.org/10.1111/j.1755-6724.2011.00456.x, 2011.

He, C. S., Dong, S. W., and Wang, Y. H.: Lithospheric delamination and upwelling asthenosphere in the Longmenshan area: insight from a teleseismic P-wave tomography, Sci. Rep., 9, 6967, https://doi.org/10.1038/s41598-019-43476-0, 2019.

He C. S., Santosh, M., Chen, X. H., and Li, X. Y.: Continental dynamics in a multi-convergent regime: a receiver function study from the North–South-Trending Tectonic Zone of China, Int. Geol. Rev., 56, 525-536, https://doi.org/10.1080/00206814.2013.876901, 2014a.

He, C. S., Santosh, M., Wu, J. P., and Chen, X. H.: Plume or no plume: Emeishan Large Igneous Province in Southwest China revisited from receiver function analysis, Phys. Earth Planet, In., 232, 72-78, https://doi.org/10.1016/j.pepi.2014.04.004, 2014b.

He, C. S., Dong, S. W., Santosh, M., and Chen, X. H.: Seismic structure of the Longmenshan area in SW China inferred from receiver function analysis: Implications for future large earthquakes, J Asian Earth Sci., 96, 226-236, https://doi.org/10.1016/j.jseaes.2014.09.026, 2014c.

He, C. S., and Santosh, M.: Crustal evolution and metallogeny in relation to mantle dynamics: A perspective from P-wave tomography of the South China Block, Lithos, 263, 3-14, https://doi.org/10.1016/j.lithos.2016.06.021, 2016.

He, C. S., and Santosh, M.: Mantle roots of the Emeishan plume: An evaluation based on teleseismic P-wave tomography, Solid Earth, 8, 1141-1151, https://doi.org/10.5194/se-2017-17, 2017a.

He, C. S., and Santosh, M.: Intraplate earthquakes and their link with mantle dynamics: Insights from P-wave teleseismic tomography along the northern part of the North–South Tectonic Zone in China, C. R. Geosci., 349, 96-105,

https://doi.org/10.5194/se-2019-119
Preprint. Discussion started: 10 July 2019

https://doi.org/10.1016/j.crte.2017.04.002, 2017b.

He, C. S., Santosh, M., and Yang, Q. Y.: Metallogeny linked to mantle dynamics in the Sanjiang Tethys region as inferred from P-wave teleseismic tomographic study, Ore Geol. Rev., 90, 1032-1041, https://doi.org/10.1016/j.oregeorev.2016.10.018, 2017.

He, C. S., and Zheng, Y. F.: Seismic evidence for the absence of deeply subducted continental slabs in the lower lithosphere beneath the Central Orogenic Belt of China, Tectonophysics, 723, 178-189, https://doi.org/10.1016/j.tecto.2017.12.018, 2018.

Hodges, K. V.: Tectonics of the Himalaya and southern Tibet from two perspectives, Geol. Soc. Am. Bull., 112, 324-350, https://doi.org/10.1130/0016-7606(2000)112<324:TOTHAS>2.0.CO;2, 2000.

Hu, J. F., Xu, X., Yang, H., Wen, L., and Li, G.: S receiver function analysis of the crustal and lithospheric structures beneath eastern Tibet, Earth Planet. Sc. Lett., 306, 77-85, https://doi.org/10.1016/j.epsl.2011.03.034, 2011.

Hu, J. F., Yang, H. Y., Xu, X. Q., Wen, L. M., and Li, G. Q.: Lithospheric structure and crust–mantle decoupling in the southeast edge of the Tibetan Plateau, Gondwana Res., 22, 1060-1067, https://doi.org/10.1016/j.gr.2012.01.003, 2012.

Huang, R. Q., Wang, Z., Pei, S. P., and Wang, Y. S.: Crustal ductile flow and its contribution to tectonic stress in Southwest China, Tectonophysics, 473, 476-489, https://doi.org/10.1016/j.tecto.2009.04.001, 2009.

Huang, Z. C, Wang, P., Xu, M. J., Wang, L. S., Ding, Z. F., Wu, Y., Xu, M. J., Mi, N., Yu. D. Y., and Li, H.: Mantle structure and dynamics beneath SE Tibet revealed by new seismic images, Earth Planet. Sc. Lett., 411, 100-111, https://doi.org/10.1016/j.epsl.2014.11.040, 2015.

Laske, G., Masters, G., Ma, Z., and Pasyanos, M. E.: CRUST1.0: an updated global model of Earth's Crust, Geophys. Res. Abstr., 14 (EGU2012-37431), 2012.

Lee, T. Y., and Lawver, L. A.: Cenozoic plate reconstruction of Southeast Asia, Tectonophysics, 251, 85-138, https://doi.org/10.1144/GSL.SP.1997.126.01.03, 1995.

Lei, J., Li, Y., Xie, F., Teng, J., Zhang, G., Sun, C., and Zha, X.: Pn anisotropic tomography and dynamics under eastern Tibetan plateau, J. Geophys. Res., 119, 2174-2198, https://doi.org/10.1002/2013JB010847, 2014.

Li, C., van der Hilst, R. D., and Toksöz, M. N.: Constraining P-wave velocity variations in the upper mantle beneath Southeast Asia, Phys. Earth Planet. In., 154, 180-195, https://doi.org/10.1016/j.pepi.2005.09.008, 2006.

Li, H. Y., Su, W., Wang, C. Y., Huang, Z. X., and Lv, Z. Y.: Ambient noise Love wave tomography in the eastern margin of the Tibetan plateau, Tectonophysics, 491, 194-204, https://doi.org/10.1016/j.tecto.2009.12.018, 2010.

Li, H. Y., Su, W., Wang, C. Y., and Huang, Z. X.: Ambient noise Rayleigh wave tomography in western Sichuan and eastern Tibet, Earth Planet. Sc. Lett., 282, 201-211, https://doi.org/10.1016/j.epsl.2009.03.021, 2009.

Li, S. L., Zhang, X. K., Zhang, C. K., Zhao, J. R., and Cheng, S. X.: A Preliminary Study on Crustal Velocity Structures of Maqin-Lanzhou-Jingbian Deep Seismic Sounding Profile, Chinese J. Geophys., 45, 209-216, https://doi.org/10.1002/cjg2.233, 2002.

Li, S. Z., Zhao, G. C., Dai, L. M., Zhou, L. H., Liu, X., Sou, Y. H., and Santosh, M.:

https://doi.org/10.5194/se-2019-119
Preprint. Discussion started: 10 July 2019

Solid Earth Discussions
Open Access

Cenozoic faulting of the Bohai Bay Basin and its bearing on the destruction of the eastern North China Craton, J. Asian Earth Sci., 47, 80-93, https://doi.org/10.1016/j.jseaes.2011.06.011, 2012.

Li, Y. L., He, J., Wang, C. S., Santosh, M., Dai, J. G., Zhang, Y. X., Wei, Y. S., and Wang, J. G.: Late Cretaceous K-rich magmatism in central Tibet: Evidence for early elevation of the Tibetan plateau?, Lithos, 160-161, 1-13, https://doi.org/10.1016/j.lithos.2012.11.019, 2013.

Li, Z. W., Ni, S. D., Hao, T. Y., Xu, Y., and Roecker, S.: Uppermost mantle structure of the eastern margin of the Tibetan plateau from interstation Pn traveltime difference tomography, Earth Planet. Sc. Lett., 335-336, 195-205, https://doi.org/10.1016/j.epsl.2012.05.005, 2012.

Li, Z. W., Ni, S. D., and Roecker, S.: Interstation Pg and Sg differential traveltime tomography in the northeastern margin of the Tibetan plateau: Implications for spatial extent of crustal flow and segmentation of the Longmenshan fault zone, Phys. Earth Planet. In., 227, 30-40, https://doi.org/10.1016/j.pepi.2013.11.016, 2014.

Liu, J. H., Liu, F. T., Wu, H., Li, Q., and Hu, G.: Three dimensional velocity images of the crust and upper mantle beneath north-south zone in China, Chinees J. Geophys., 95, 916-925, https://doi.org/10.1785/0120010130, 1989.

Lü, Y., Zhang, Z. J., Pei, S. P., Sandvol, E., Xu, T., and Liang, X. F.: 2.5-Dimensional tomography of uppermost mantle beneath Sichuan–Yunnan and surrounding regions, Tectonophysics, 627, 193-204, https://doi.org/10.1785/0120010130, 2014.

Lustrino, M.: How the delamination and detachment of lower crust can influence basaltic

https://doi.org/10.5194/se-2019-119
Preprint. Discussion started: 10 July 2019

magmatism, Earth-Sci. Rev., 72, 21-38, https://doi.org/10.1016/j.earscirev.2005.03.004, 2005.

Metcalfe, I.: Gondwana dispersion and Asian accretion: tectonic and palaeogeographic evolution of eastern Tethys, J. Asian Earth Sci., 66, 1-33, https://doi.org/10.1016/j.jseaes.2012.12.020, 2013.

Mo, X. X., Deng, J. F., Dong, F. L., H, Y. X., Wang, Y., Zhou, S., and Yang, W. G.: Volcanic petrotectonic assemblages in Sanjiang Orogenic Belt, SW China and implication for tectonics, Geol. J. China Univ., 7, 121-138 (in Chinese with English abstract), 2001.

Rowley D. B.: Minimum age of initiation of collision between India and Asia north of Everest based on the subsidence history of the Zhepure Mountain section, J. Geol., 106, 229-35, https://doi.org/10.1086/516018, 1998.

Paige, C. C., and Saunders, M. A.: LSQR: an algorithm for sparse linear equations and spare least squares, ACMTrans. Math. Softw., 8, 43-71, https://doi.org/10.1145/355984.355989, 1982.

Peate, I. U., and Bryan, S. E.: Re-evaluating plume-induced uplift in the Emeishan large igneous province, Nat. Geosci., 1, 625-629, https://doi.org/10.1038/ngeo281, 2008.

Pirajno, F.: Ancient to modern earth: the role of mantle plumes in the making of continental crust, In: Earth's Oldest Rocks, edited by Martin, J., Van Kranendonk, R. H. S., and Vickie, C. B., Develop. Preca. Geol., 15, 1037-1064, https://doi.org/10.1016/S0166-2635(07)15083-0, 2007.

Replumaz, A., Negredo, A. M., Guillot, S., and Villaseñor, A.: Multiple episodes of

https://doi.org/10.5194/se-2019-119
Preprint. Discussion started: 10 July 2019

continental subduction during India/Asia convergence: insight from seismic tomography and tectonic reconstruction, Tectonophysics 483, 125-134, https://doi.org/10.1016/j.tecto.2009.10.007, 2010.

Royden, L. H., Burchfiel, B. C., and van der Hilst, R. D.: The geological evolution of the Tibetan plateau, Science, 321, 1054-1058, https://doi.org/10.1126/science.1155371, 2008.

Rudnick, R. L.: Making continental crust, Nature 378, 571-578, https://doi.org/10.1038/378571a0, 1995.

Santosh, M., Maruyama, S., Komiya, T., and Yamamoto, S.: Orogens in the evolving Earth: from surface continents to 'lost continents' at the core-mantle boundary, Geol. Soci. Lond. Spec. Pub., 338, 77-116, https://doi.org/10.1144/SP338.5, 2010.

Silver, P. G., Behn, M. D., Kelley, K., Schmitz, M., and Savage, B.: Understanding cratonic flood basalts, Earth Planet. Sc. Lett., 245, 190-201, https://doi.org/10.1016/j.epsl.2006.01.050, 2006.

Sol, S., Meltzer, A., Burgmann, R., van der Hilst, R. D., King, R., Chen, Z., Koons, P. O., Lev, E., Liu, Y. P., Zeitler, P. K., Zhang, X., Zhang, J., and Zurek, B.: Geodynamics of the southern Tibetan Plateau from seismic anisotropy and geodesy, Geology, 35, 563-566, https://doi.org/10.1130/g23408a.1, 2007.

Tapponnier, P., Xu, Z., Roger, F., Meyer, B., Arnaud, N., Wittlinger, G., and Yang, J.: Oblique stepwise rise and growth of the Tibet plateau, Science, 294, 1671-1677, https://doi.org/10.1126/science.105978, 2001.

Ueda, K., Gerya, T. V., and Burg, J. P.: Delamination in collisional orogens:

https://doi.org/10.5194/se-2019-119
Preprint. Discussion started: 10 July 2019

Thermomechanical modeling, J. Geophys. Res., 117, B08202, https://doi.org/10.1029/2012JB009144, 2012.

VanDecar, C., and Crosson, S.: Determination of teleseismic relative phase arrival times using multi-channel cross-correlation and least squares, B. Seismol. Soc. Am., 80, 150-169, https://doi.org/10.1016/0040-1951(90)90194-D, 1990.

Wang, C. S., Gao, R., Yin, A., Wang, H. Y., Zhang, Y. X., Guo, T. L., Li, Q. S., and Li, Y. L.: A mid-crustal strain-transfer model for continental deformation: A new perspective from high-resolution deep seismic-reflection profiling across NE Tibet, Earth Planet. Sc. Lett., 306, 279-288, https://doi.org/10.1016/j.epsl.2011.04.010, 2011.

Wang, C. Y., Flesch, L. M., Silver, P. G., Chang, L. J., and Chan, W. W.: Evidence for mechanically coupled lithosphere in central Asia and resulting implications, Geology, 36, 363-36, https://doi.org/10.1130/G24450A.1, 2008.

Wang, H. Y., Gao, R., Zeng, L. S., Kuang, Z. Y., Xue, A. M., Li, W. H. Xiong, X. S., and Huang, W. Y.: Crustal structure andMoho geometry of the northeastern Tibetan plateau as revealed by SinoProbe-02 deep seismic-reflection profiling, Tectonophysics, 636, 32-39, https://doi.org/10.1016/j.tecto.2014.08.010, 2014.

Wu, Y. B., and Zheng, Y. F.: Tectonic evolution of a composite collision orogen: An overview on the Qingling-Tongbai-Hong'an-Dabie-Sulu orogenic belt in central China, Gondwana Res., 23, 1402-1428, https://doi.org/10.1016/j.gr.2012.09.007, 2013.

Xiao, L., Xu, Y. G., Mei, H. J., Zheng, Y. F., He, B., and Pirajno, F.: Distinct mantle sources of low-Ti and high-Ti basalts from the western Emeishan large igneous

https://doi.org/10.5194/se-2019-119
Preprint. Discussion started: 10 July 2019

Solid Earth Discussions

province, SW China: implications for plume–lithosphere interaction, Earth Planet. Sc. Lett., 228, 525-546, https://doi.org/10.1016/j.epsl.2004.10.002, 2004.

Xu, X. X. Tan, X. B., Yu, G. H., Wu, G. D., Fang, W., Chen, J. B., Song, H. P., and Shen, S.: Normal- and oblique-slip of the 2008 Yutian earthquake: Evidence for eastward block motion, northern Tibetan Plateau, Tectonophysics, 152-165, https://doi.org/10.1016/j.tecto.2012.08.007, 2013.

Xu, Y. G., He, B., Chung, S. L., Menzies, M., and Frey, F. A.: Geologic, geochemical, and geophysical consequences of plume involvement in the Emeishan flood-basalt province, Geology, 32, 917-920, https://doi.org/10.1130/G20602.1, 2004.

Xu, Y. G., He, B., Huang, X. L., Luo, Z. Y., Chung, S. L., Xiao, L., Zhu, D., Shao, H., Fan, W. M., Xu, J. F., and Wang, Y. J.: Identification of mantle plumes in the Emeishan Large Igneous Province, Episodes, 30, 32-42, https://doi.org/10.1007/s00254-006-0532-6, 2007.

Xu, Y., Yang, X. T., Li, Z. W., and Liu, J. H.: Seismic structure of the Tengchong volcanic area southwest China from local earthquake tomography, J. Volcanol. Geoth. Res., 239-240, 83-91, https://doi.org/10.1016/j.jvolgeores.2012.06.017, 2012.

Xu, Z. Q., Yang, J. S., Wu, C. L., and Li, H. B.: Timing and mechanism of formation and exhumation of the Northern Qaidam ultrahigh-pressure metamorphic belt, J Asian Earth Sci., 28, 160-173, https://doi.org/10.1016/j.jseaes.2005.09.016, 2006.

Yang, T., Wu, J. P., Fang, L. H., and Wang, W. L.: Complex Structure beneath the Southeastern Tibetan Plateau from Teleseismic P-Wave Tomography, B. Seismol. Soc. Am., 104, 1056-1069, https://doi.org/10.1785/0120130029, 2014.

Yang, J. S., Xu Z. Q, Dobrzhinetskaya, L. F., Green II, H. W., Pei, X. Z., Shi, R. D., Wu, C. L., Wooden, J. L., Zhang, J. X., Wan, Y. S., and Li, H. B.: Discovery of metamorphic diamonds in central China： an indication of a >4000·km·long zone of deep subduction resulting from mutiple continental collisions, Terra Nova, 15, 370-379, https://doi.org/10.1046/j.1365-3121.2003.00511.x, 2003.

Zhang, C. Z., Li, B., Cai, J. X., Tang, X. C., Wei, Q. G., and Zhang, Y. X.: A-type granite and adakitic magmatism association in Songpan-Garze fold belt, eastern Tibetan Plateau: Implicaiton for lithospheric delamination, Lithos, 103, 562-564, https://doi.org/10.1016/j.lithos.2007.09.021, 2008.

Zhang, K. J., Xia, B. D., Wang, G. M., Li, Y. T., and Ye, H. F.: Early Cretaceous stratigraphy, depositional environments, sandstone provenance, and tectonic setting of central Tibet, western China, Geol. Soc. Am. Bull., 116, 1202-1222, https://doi.org/10.1130/B25388.1, 2004.

Zhang, K. J.: Is the Songpan-Ganzi terrane (central China) really underlain by oceanic crust?, J. Geol. Soc. India, 57, 233-230, 2001.

Zhang, P. Z.: A review on active tectonics and deep crustal processes of the Western Sichuan region, eastern margin of the Tibetan Plateau, Tectonophysics, 584, 7-22, https://doi.org/10.1016/j.tecto.2012.02.021, 2013.

Zhang, P. Z., Deng, Q., Zhang, G., Ma, J., and Gan, W.: Active tectonic blocks and strong earthquakes in continental China, Sci. China Ser. D, 33, 13-24 (Suppl.), https://doi.org/10.1360/03dz0002, 2003.

Zhao, D.: Global tomogaphic images of mantle plumes and subducting slabs: insight into

https://doi.org/10.5194/se-2019-119
Preprint. Discussion started: 10 July 2019

deep Earth dynamics, Phys. Earth Planet. In., 146, 3-34, https://doi.org/10.1016/j.gca.2006.06.1331, 2004.

Zhao, D., Hasegawa, A., and Horiuchi, S.: Tomographic imaging of P- and S-wave velocity structure beneath northeastern Japan, J. Geophys. Res., 97, 19909-19928, https://doi.org/10.1029/92JB00603, 1992.

Zhao, D., Hasegawa, A., and Kanamori, H.: Deep structure of Japan subduction zones as derived from local, regional, and teleseismic events, J. Geophys. Res., 99, 22313-22329, https://doi.org/10.1029/94JB01149, 1994.

Zhao, D., and Ohtani, E.: Deep slab subduction and dehydration and their geodynamic consequences: evidence from seismology and mineral physics, Gondwana Res., 16, 401-413, https://doi.org/10.1016/j.gr.2009.01.005, 2009.

Zhao, X., Xiao, W., Hebert, R., and Wang, C.: Plate tectonics of Asia: Geological and geophysical constraints, Gondwana Res., 22, 353-359, https://doi.org/10.1016/j.gr.2012.01.002, 2012.

Zhu, D. C., Zhao, Z. D., Niu, Y. L., Mo, X. X., Chung, S. L., Hou, Z. Q., Wang, L. Q., and Wu, F. Y.: The Lhasa Terrane. Record of a microcontinent and its histories of drift and growth, Earth Planet. Sc. Lett., 301, 241-255, https://doi.org/10.1016/j.epsl.2010.11.005, 2011.